Catalysis Communications 118 (2019) 56–59

Contents lists available at ScienceDirect

Catalysis Communications

journal homepage: www.elsevier.com/locate/catcom

Short communication

Hindered methane decomposition on a coke-resistant Ni-In/SiO_2 dry reforming catalyst

Miklós Németh[a], György Sáfrán[b], Anita Horváth[a], Ferenc Somodi[a,*]

[a] Hungarian Academy of Sciences, Centre for Energy Research, Institute for Energy Security and Environmental Safety, Department of Surface Chemistry and Catalysis, Konkoly-Thege M. street 29-33, H-1121 Budapest, Hungary

[b] Hungarian Academy of Sciences, Centre for Energy Research, Institute for Technical Physics and Materials Science, Konkoly-Thege M. street 29-33, H-1121 Budapest, Hungary

ARTICLE INFO

Keywords:
Methane decomposition
Dry reforming
Silica supported nickel catalyst
Nickel-indium bimetallic catalyst
Coke formation

ABSTRACT

Decomposition of methane has been investigated by mass spectrometry assisted pulse chemisorption experiments at 600 °C on freshly reduced and on carburized Ni/SiO_2 and Ni-In/SiO_2 dry reforming catalysts. The results showed complete methane decomposition with stoichiometric hydrogen production on freshly reduced Ni/SiO_2, while strong hydrogen chemisorption and partial methane decomposition was observed on Ni-In/SiO_2. Hydrogen production decreased on both carburized catalysts and dissociative methane chemisorption without hydrogen formation was observed on the bimetallic catalyst. This difference in methane activation might be one of the reasons for the absence of coke on the bimetallic catalyst during dry reforming of methane.

1. Introduction

Carbon dioxide reforming of methane (dry reforming of methane, DRM, $CO_2 + CH_4 \rightleftharpoons 2\ CO + 2\ H_2$) has been intensively studied in the last two decades because of its potential in utilization of these greenhouse gases, in direct conversion of biogas and CO_2 containing natural gas [1]. The produced mixture of carbon monoxide and hydrogen (synthesis gas) can be further converted by Fischer-Tropsch synthesis to other important chemicals such as methanol, and synthetic fuels [2]. In spite of the above prospects, DRM hasn't reached industrial scale application [3] because the commercially feasible supported nickel catalysts are prone to deactivating carbon formation when the reaction conditions aren't optimal (temperature is lower than 870–1040 °C and the CH_4/CO_2 ratio is larger than 1 [4]). The inactive carbon deposited on the catalyst surface during DRM comes from two side reactions: methane decomposition and CO disproportionation. The dissociation of CH_4 on transition metal surfaces undergoes via the formation of CH_x (x: 0–4) species multiply bonded to the surface [5]. In the case of complete dissociation, carbon atoms may diffuse into the metal particle or polymerize on its surface forming various carbonaceous structures [6,7]. Therefore, one of the strategies against coking is the modification of the active metal surface with other elements [8–12] to inhibit the formation of multiple bonded carbon species. Following this approach, we have recently shown that on a nickel-indium bimetallic catalyst carbon formation is inhibited during DRM [13].

The goal of the present study is to provide a deeper insight into the surface processes during methane chemisorption at working temperature (600 °C) of the silica supported monometallic Ni and bimetallic Ni-In dry reforming catalysts used in our previous study [13]. Five methane pulses (0.16 μmol each) were added to the freshly reduced catalysts, and to catalysts after 1 min and after 1 h continuous flow of methane (1%CH_4-He) (partially and extensively carburized samples, respectively). QMS was used to analyze the products and the remaining reactants and based on the calculated mass balance, the composition of chemisorbed surface species after each methane pulses was calculated. To analyze the carbonaceous structures after 1 h CH_4 flow, temperature-programmed oxidation (TPO), and HRTEM and XPS measurements were carried out.

2. Experimental

2.1. Catalyst preparation

3wt%Ni/SiO_2 and 3wt%Ni-2wt%In/SiO_2 catalysts were prepared by deposition-precipitation with urea. The detailed description of the catalyst preparation and the results of their characterization can be found elsewhere [13].

* Corresponding author.
E-mail address: somodi.ferenc@energia.mta.hu (F. Somodi).

https://doi.org/10.1016/j.catcom.2018.10.003
Received 22 June 2018; Received in revised form 24 September 2018; Accepted 2 October 2018
Available online 04 October 2018

2.2. Pulse-flow experiments

Pulse-flow experiments were conducted using an automated catalyst characterization station (Autochem II 2920) equipped with a ThermoStar quadrupol mass spectrometer. 46.2 mg of the dried monometallic and 52.3 mg of the bimetallic catalyst was placed in a quartz U-tube reactor. First, the sample was calcined at 700 °C for 1 h in flowing 10% O2-He atmosphere. After cooling down to room temperature in helium flow, the sample was reduced in flowing 10%H_2-Ar mixture at 700 °C. After one hour at this temperature, the gas flow was changed to He and the sample was cooled to 600 °C where 5 pulses (0.5 cm^3 each) of 1%CH_4-He was injected into the He flow. The composition of the outlet gas flow was analyzed by the mass spectrometer. Then 1 min continuous flow of 1%CH_4-He at 50 ml/min was used to build more carbon deposits (partially carburized surface). The experiment was continued by 5 pulses of 1%CH_4-He, then the sample was cooled down to room temperature in flowing He, and temperature-programmed oxidation (TPO) was used to further characterize the carbon deposits. During TPO, the sample was heated to 700 °C in 10% O_2-He for 1 h and mass spectrometer was used to detect the evolved CO_2. During the experiments, the heating rate was 10 °C/min and the gas flows were 50 ml/min except the TPO experiments, where 30 ml/min was used. (MS spectra of 1%CH_4-He pulses can be seen in Fig. S1).

This whole experimental sequence was then repeated without removing the catalyst from the sample tube, except that instead of 1 min, 1 h 1%CH_4-He flow was used to create an extensively carburized surface. After 1 h methane flow, before TPO experiments, the catalysts surface was analyzed by HRTEM. To the sake of brevity, Table S1 summarizes the measurement sequence.

2.3. X-ray photoelectron spectroscopy

For the determination of surface composition and oxidation state of the metals, X-ray photoelectron spectroscopy (XPS) measurements were done using a KRATOS XSAM 800 XPS machine equipped with an atmospheric reaction chamber. Al K_α characteristic X-ray line, 40 eV pass energy and FAT mode were applied for recording the XPS lines of Ni 2p, O 1 s, In 3d, C 1 s, Si 2p regions. Si 2p binding energy at 103.5 eV was used as reference for charge compensation.

2.4. Transmission electron microscopy

The morphology of the catalysts after 1 h of methane flow were studied by a JEOL 3010 high resolution transmission electron microscope operating at 300 kV. Histograms of the particle size distribution were obtained by counting at least 300 particles; the mean particle diameter (d_m) was calculated by using the formula $d_m = \Sigma d_i n_i / \Sigma_i n_i$ where ni was the number of particles of diameter d_i.

3. Results and discussion

The product distributions of each methane pulses obtained on freshly reduced (Fig. 1A and D), on partially carburized (Fig. 1B and E) and extensively carburized (Fig. 1C and F) surface clearly showed the difference in the methane activation ability of the two catalysts, namely, the amount of hydrogen produced during methane pulses significantly differed on the two catalysts. On Ni/SiO_2, complete methane conversion was observed on the freshly reduced and partially carburized catalyst (Fig. 1A and B). After 1 h methane flow (Fig. 1C), the amount of hydrogen significantly decreased due to the limited methane dissociation on the extensively carburized surface. In the case of Ni-In/SiO_2 catalyst, as opposed to the Ni/SiO_2, the methane dissociation was limited on each surface (Fig. 1D and E) and the hydrogen production completely diminished on the extensively carburized surface (Fig. 1F). CO and CO_2 was observed in the gas phase during methane pulses on both freshly reduced catalysts. This suggests the contribution of the surface OH groups situated in the close vicinity of catalytically active sites [14,15]. Although the concentration of hydroxyl groups on the silica surface significantly decreases after heat treatment at 700 °C, they are still exist on the surface [16]. According to the literature, the OH-group concentration after heat treatment at 700 °C can be 1–2 OH/nm^2 [17]. Presumably, the number of these OH groups further decreases upon longer exposure to methane which explains the lack of CO and CO_2 in the product streams when methane pulses were added to carburized catalysts.

Based on the mass balance of the methane pulses, provided by the on-line mass spectroscopy detection, the methane consumption and H/C ratio of the chemisorbed species retained on the surface after the methane pulses could be determined (Table 1). On the Ni-In/SiO_2 catalyst, the obtained high conversion and the low amount of hydrogen produced, suggested the presence of partially dissociated methane and hydrogen atoms unable to recombine to molecules on the catalyst surface. The CH_4 conversion of the pulses was the highest on both freshly reduced catalysts. The conversion decreased when pulses were added to partially carburized (after 1 min CH_4 flow) and extensively carburized (after 1 h CH_4 flow) surfaces showing that the amount of catalytically active sites decreased due to carbon deposition on the surface of metal particles.

Based on the before mentioned H/C ratios obtained after each methane pulses added to differently carburized catalysts, the stoichiometry of chemisorbed species could be determined. The schematic illustrations of adsorbed species are shown in Scheme S1.

All of the methane was consumed by the freshly reduced Ni/SiO_2, in other words stoichiometric amount of hydrogen was produced and appeared in the gas phase and only small amount of carbon remained on the surface after each CH_4 pulses (Scheme S1A). On the bimetallic catalyst, in parallel with the low hydrogen production and high CH_4 conversion, the H/C ratio on the surface was higher than 4, suggesting the coexistence of adsorbed hydrogen and partially dissociated methane ($-CH_x$, x:1–3) on the metal particles (Scheme S1D). These results show prompt hydrogen recombination and desorption on nickel, and strong hydrogen chemisorption on the bimetallic surface. Consequently, the apparent stoichiometry of the chemisorbed $-CH_x$ species on the bimetallic surface cannot be determined based on the surface H/C ratio. Since the exact number of chemical bonds by which the $-CH_x$ species are attached to the bimetallic surface is unknown, it is also difficult to determine the $-CH_x$ coverage. However, the amount of chemisorbed methane compared to the number of available surface sites after 5 methane pulses can be estimated - for the sake of simplicity – on the freshly reduced bimetallic surface. Based on the nickel content (3 wt%) and dispersion (11.7%) determined by CO pulse chemisorption in [13], the amount of available surface sites can be calculated using the weight of the catalyst bed (0.0523 g): It is 3.13 μmol Ni. One methane pulse contains 0.16 μmol CH_4. Knowing that the methane conversion is about 92% of each pulses, $5 \times 0.16 \times 0.92 = 0.74$ μmol CH_4 stays on the surface in the form of $-CH_x$ after 5 methane pulses. This is about four times lower than the amount of available surface sites, but again, the exact stoichiometry of the surface species is unknown, so the coverage, that is what percent of the available surface is occupied by $-CH_x$ species, cannot be determined.

On partially carburized Ni/SiO_2 catalyst (after 1 min CH_4 flow), the amount of carbon deposited during methane pulses was about three times higher than that of the hydrogen, which implied the presence of surface carbon atoms and ≡CH adsorbed species (Scheme S1B). On the Ni-In/SiO_2, the H/C ratio was close to 4, which based on the above, suggested that partially dissociated methane ($-CH_x$, x: 1–3) and hydrogen populated the surface. (Scheme S1E).

On extensively carburized Ni/SiO_2 catalyst (after 1 h CH_4 flow), the H/C ratio on the surface after each methane pulses was around 3, therefore the plausible adsorbed species were mostly $-CH_3$. This results shows that the number of surface sites available for the C–H bond cleavage decreased due to the presence of carbon on the surface after

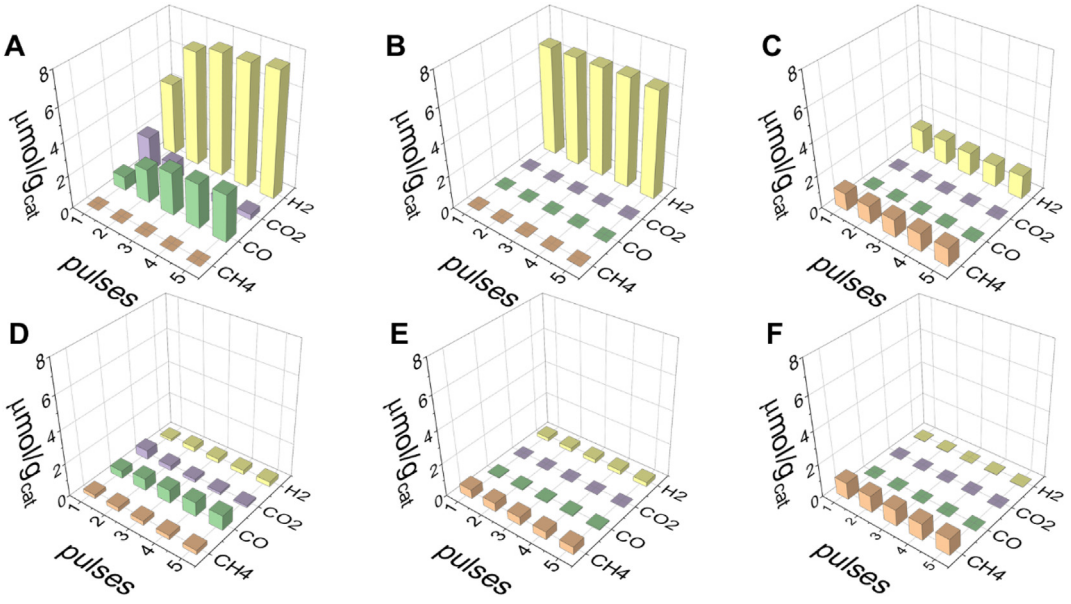

Fig. 1. Product distributions of methane impulses on freshly reduced Ni/SiO_2 catalysts (A), after 1 min flow of methane (B), after 1 h flow of methane (C). Product distributions of methane impulses on freshly reduced $Ni\text{-}In/SiO_2$ catalysts (D), after 1 min flow of methane (E), after 1 h flow of methane (F).

Table 1
Product distribution and derived data of the 5th pulse of methane added to freshly reduced, partially carburized (1 min CH_4 flow) and extensively carburized (1 h CH_4 flow) Ni/SiO_2 and $Ni\text{-}In/SiO_2$ catalysts.

	CH_4[a]	CO[a]	CO_2[a]	H_2[a]	C_{surf}[b]	H_{surf}[c]	CH_4 conv[d]	H_{surf}/C_{surf}
Ni/SiO_2								
Freshly reduced	0.00	2.87	0.33	7.46	0.27	0.00	1.00	n.a.
After 1 min CH_4 flow	0.01	0.00	0.00	6.38	3.46	1.05	1.00	0.30
After 1 h CH_4 flow	1.11	0.01	0.00	1.42	2.35	6.58	0.68	2.81
$Ni\text{-}In/SiO_2$								
Freshly reduced	0.26	0.89	0.11	0.29	1.80	10.62	0.92	5.91
After 1 min CH_4 flow	0.47	0.05	0.00	0.27	2.54	9.83	0.85	3.88
After 1 h CH_4 flow	0.98	0.00	0.00	0.02	2.08	8.27	0.68	3.99

[a] amount of gases in the outlet after the methane pulse in ($\mu mol/g_{cat}$).
[b] amount of carbon ($\mu mol/g_{cat}$) remained on the surface after CH_4 pulses calculated from the mass balance of the methane pulse containing 0.16 μmol CH_4.
[c] amount of hydrogen ($\mu mol/g_{cat}$) remained on the surface after CH_4 pulses calculated from the mass balance of the methane pulse containing 0.16 μmol CH_4.
[d] conversion calculated from the molar amount of methane in the inlet and outlet flows of the reactor tube using the following formula: $(CH_4^{in}\text{-}CH_4^{out})/CH_4^{in}$.

1 h of CH_4 flow. (Scheme S1C). The H/C ratio on the bimetallic catalyst remained around 4 without hydrogen production. The considerable methane uptake suggested the sole presence of partially dissociated methane ($-CH_x$, x: 1–3) and hydrogen on the surface (Scheme S1F).

Based on the above findings, it is not easy to correlate the different methane decomposition ability of the catalysts with their activity in DRM, because DRM is a rather complex reaction. During DRM, carbon dioxide is also present and activated on the surface, providing CO and an oxygen atom. According to the literature, $-CH_x$ species may react with the above mentioned oxygen species and with surface hydroxyl groups on the support to yield CO and H_2. The exact reaction mechanism may depend on the type of metal and support used in the reaction [18]. In spite of the fact that the methane dissociation on the two catalysts is very different, in our previous work it was shown that there was no significant difference in the catalytic activity of the two catalysts during DRM [13]. The only prominent difference between the two catalysts was the lack of surface carbon formation on the bimetallic catalyst.

The amount of carbon deposited during 1 min and 1 h methane flows determined by TPO (Fig. S2) was 174.5 and 428.9 $\mu mol/g_{cat}$ for the monometallic and 14.0 and 254.3 $\mu mol/g_{cat}$ for the bimetallic catalyst, which also represented the hindered methane decomposition on the bimetallic catalyst. The TPO peaks were positioned at around 330–350 °C on both catalysts suggesting the presence of carbonaceous species, most likely situated on the metal particles. This was supported by TEM results after 1 h CH_4 flow (Fig. S3A and S3B), that is carbon nanotubes or nanofibers which oxidation requires temperatures higher than 350 °C [19], were not observed. It is worth noting that the average particle size of the two catalysts was comparable after reduction, 1.8 nm and 2.9 nm for the monometallic and for the bimetallic catalyst, respectively. Furthermore, previous XPS measurements showed that the Ni/In surface ratio is 2.2 [13], which suggested decreased number of Ni atoms available for methane decomposition compared to the monometallic catalyst. However, the methane conversion (or methane uptake, since there is minimal hydrogen formation observed on the bimetallic catalyst) of the bimetallic catalyst did not differ very much from the monometallic catalyst, that is the active metal surface area was not significantly different on the two catalysts. Based on the above mentioned facts, the lower amount of carbon deposition on the bimetallic catalyst was not caused by decreased metal surface area of nickel, but rather by the lower decomposition rate, since the hydrogen formation was much less on bimetallic catalyst. Note that, the decomposition rate is strongly influenced by the type of chemisorption which is affected by the presence of indium on the surface.

The average particle size increased on both catalysts after 1 h methane flow, but the magnitude of the change was larger on Ni/SiO_2: the average particle size of 1.8 nm of the reduced catalyst [13] increased to 3.0 nm, the value of $Ni\text{-}In/SiO_2$ changed from 2.9 nm [13] to 3.2 nm. Carbon atoms formed during methane decomposition might have been diffused into the metal particles [20] inducing the increase of average particle size. Accordingly, nickel carbide (Ni_xC) was found on Ni/SiO_2 by HRTEM (Fig. S4). In the HRTEM image of $Ni\text{-}In/SiO_2$, the

determined interplanar spacings were in consonance with our previous study [13] and corresponded to Ni_2In alloy, however nickel carbide particles were not observed (Fig. S5). To further analyze the surface carbon deposited on the catalysts during 1 h CH_4 flow, XPS measurements were done (Fig. S6). The higher amount of surface carbon on Ni/SiO_2 was not reflected in the results, that is, the calculated C/Si ratio was 0.12 and 0.13 for the monometallic and for the bimetallic catalyst respectively. The C 1 s XP spectra of the two catalysts were quite similar, both spectra had three components: Ni_xC around 281.8 eV, sp2 carbon at 284.1 eV and a C—O component at 285.9 eV [21]. The binding energy of Ni $2p_{3/2}$ photoelectron peaks (852.2 eV for the Ni/SiO_2 and 852.4 eV for the Ni-In/SiO_2), were in good agreement with our previous results [13], nickel carbide component was not observed. The difference in the binding energy of Ni 2p3/2 peaks was 0.2 eV, based on which solid conclusion cannot be drawn concerning the effect of indium on nickel chemical state. It was shown in our previous study by XPS, that the presence of indium only slightly affected the chemical state of nickel after reduction at 700 °C [13]. However, based on the higher affinity of hydrogen to the bimetallic catalyst observed in the present study, we think that indium not only modifies the structure of the available adsorption sites but also has an electronic effect on the nickel surface which strongly affects the chemisorption.

4. Conclusions

In summary, decomposition of methane has been investigated by MS assisted methane pulse chemisorption experiments at 600 °C using freshly reduced, partially carburized and extensively carburized Ni/SiO_2 and Ni-In/SiO_2 catalysts. It was found that hydrogen production during CH_4 pulses decreased on both catalysts as the extent of carburization of the surface increased. Under our experimental conditions, formation of various carbonaceous structures separated from the metal particles was not observed by TPO and HRTEM measurements, however it was pointed out that carbon atoms diffused into the metal nanoparticles. It was shown that the presence of surface carbon on Ni/SiO_2 significantly changed the hydrogen content of chemisorbed species obtained upon CH_4 impulses. Methane chemisorption was only slightly affected by the surface carbon content on Ni-In/SiO_2, the H/C ratio of the surface species was equal to or higher than 4 during the experiments. Based on the high H/C ratio of surface species and the low hydrogen production and limited carbon formation of the bimetallic catalyst, the role of indium in methane decomposition is twofold: First, it changes the surface structure of adsorption sites so that the complete dissociation of methane is hindered. Secondly, it has an electronic effect on nickel which leads to stronger hydrogen chemisorption compared to the monometallic catalyst. This difference in methane activation might be one of the responsible factors for the coke-free operation of the bimetallic catalyst during dry reforming of methane.

Acknowledgement

The financial support and the Postdoctoral Scholarship provided by the Hungarian National Research Fund [OTKA PD#116384] is greatly acknowledged. The authors are thankful to Dr. Claudio Evangelisti for his help and comments concerning the HRTEM results. The authors are grateful to Dr. Antal Tungler and to Dr. Andrea Beck for her overall comments and suggestions.

Appendix A. Supplementary data

Supplementary data to this article can be found online at https://doi.org/10.1016/j.catcom.2018.10.003.

References

[1] M.C.J. Bradford, M.A. Vannice, CO2 Reforming of CH4, Catal. Rev. 41 (1999) 1–42.
[2] M.-S. Fan, A.Z. Abdullah, S. Bhatia, Catalytic technology for carbon dioxide reforming of methane to synthesis gas, ChemCatChem 1 (2009) 192–208.
[3] P. Gangadharan, K.C. Kanchi, H.H. Lou, Evaluation of the economic and environmental impact of combining dry reforming with steam reforming of methane, Chem. Eng. Res. Des. 90 (2012) 1956–1968.
[4] S. Wang, G.Q.M. Lu, G.J. Millar, Carbon dioxide Reforming of methane to produce synthesis gas over metal-supported catalysts: state of the art, Energy Fuel 10 (1996) 896–904.
[5] M.-S. Liao, Q.-E. Zhang, Dissociation of methane on different transition metals, J. Mol. Catal. A Chem. 136 (1998) 185–194.
[6] M.V. Kharlamova, Investigation of growth dynamics of carbon nanotubes, Beilstein J. Nanotechnol. 8 (2017) 826–856.
[7] S. Hofmann, R. Sharma, C. Ducati, G. Du, C. Mattevi, C. Cepek, M. Cantoro, S. Pisana, A. Parvez, F. Cervantes-Sodi, A.C. Ferrari, R. Dunin-Borkowski, S. Lizzit, L. Petaccia, A. Goldoni, J. Robertson, In situ observations of catalyst dynamics during surface-bound carbon nanotube nucleation, Nano Lett. 7 (2007) 602–608.
[8] C. Liu, J. Ye, J. Jiang, Y. Pan, Progresses in the preparation of coke resistant Ni-based catalyst for steam and CO2 reforming of methane, ChemCatChem 3 (2011) 529–541.
[9] A. Horváth, L. Guczi, A. Kocsonya, G. Sáfrán, V. La Parola, L.F. Liotta, G. Pantaleo, A.M. Venezia, Sol-derived AuNi/MgAl2O4 catalysts: Formation, structure and activity in dry reforming of methane, Appl. Catal. A Gen. 468 (2013) 250–259.
[10] M. Németh, D. Srankó, J. Károlyi, F. Somodi, Z. Schay, G. Sáfrán, I. Sajó, A. Horváth, Na-promoted Ni/ZrO_2 dry reforming catalyst with high efficiency: details of Na_2O–ZrO_2–Ni interaction controlling activity and coke formation, Catal. Sci. Technol. 7 (2017) 5386–5401.
[11] J.R. Rostrupnielsen, J.H.B. Hansen, CO2-Reforming of methane over transition Metals, J. Catal. 144 (1993) 38–49.
[12] E. Nikolla, A. Holewinski, J. Schwank, S. Linic, Controlling carbon surface chemistry by alloying: carbon tolerant reforming catalyst, J. Am. Chem. Soc. 128 (2006) 11354–11355.
[13] J. Károlyi, M. Németh, C. Evangelisti, G. Sáfrán, Z. Schay, A. Horváth, F. Somodi, Carbon dioxide reforming of methane over Ni–In/SiO2 catalyst without coke formation, J. Ind. Eng. Chem. 58 (2018) 189–201.
[14] P. Ferreira-Aparicio, I. Rodríguez-Ramos, A. Guerrero-Ruiz, Methane interaction with silica and alumina supported metal catalysts, Appl. Catal. A Gen. 148 (1997) 343–356.
[15] T.V. Choudhary, C. Sivadinarayana, C.C. Chusuei, A. Klinghoffer, D.W. Goodman, Hydrogen production via catalytic decomposition of methane, J. Catal. 199 (2001) 9–18.
[16] A. Feng, B.J. McCoy, Z.A. Munir, D.E. Cagliostro, Water adsorption and desorption kinetics on silica insulation, J. Colloid Interface Sci. 180 (1996) 276–284.
[17] C.J. Brinker, G.W. Scherer, Sol-gel science: the physics and chemistry of sol-gel processing, Academic Press, Boston, 1990.
[18] D. Pakhare, J. Spivey, A review of dry (CO2) reforming of methane over noble metal catalysts, Chem. Soc. Rev. 43 (2014) 7813–7837.
[19] C. Pham-Huu, N. Keller, V.V. Roddatis, G. Mestl, R. Schlögl, M.J. Ledoux, Large scale synthesis of carbon nanofibers by catalytic decomposition of ethane on nickel nanoclusters decorating carbon nanotubes, Phys. Chem. Chem. Phys. 4 (2002) 514–521.
[20] D.L. Trimm, The formation and removal of coke from nickel catalyst, Catal. Rev. 16 (1977) 155–189.
[21] I. Czekaj, F. Loviat, F. Raimondi, J. Wambach, S. Biollaz, A. Wokaun, Characterization of surface processes at the Ni-based catalyst during the methanation of biomass-derived synthesis gas: X-ray photoelectron spectroscopy (XPS), Appl. Catal. A Gen. 329 (2007) 68–78.